Defence Science Journal, Vol. 68, No. 4, July 2018, pp. 337-342, DOI : 10.14429/dsj.68.10433

Passive Thermal Management of Launch Vehicle Systems using Phase Changing Materials

V.K. Sen*, J. Jaiswal, A. Nandi, A.V. Aliyas, and A. Pillai

Vikram Sarabhai Space Centre, Trivandrum - 695 022, India
**E-mail: vijay_sen@vssc.gov.in*

ABSTRACT

Electronic systems in expendable launch vehicles and missiles rely on their own thermal inertia to operate for the stipulated time, without overheating, owing to absence of active cooling systems and natural convection at elevated altitude. Traditionally, this inertia is built-into the electronics by increasing its chassis (support structure) mass, proportional to the associated thermal load. For power intensive systems, especially in vehicle upper stages where mass is at premium, this approach results in proportional reduction in payload capability. In the present paper, a heat sink based on Neopentyl Glycol (NPG) with solid-to-solid phase change (crystalline transformation) is explored as a mass effective alternative due to its capability to absorb a significant amount of energy during phase change. However, due to its lower thermal conductivity, a thermal conductivity enhancer (TCE) to maximise heat transfer is essential. The resulting heat sink, utilising TCE for heat distribution and NPG for heat storage can be called hybrid heat sink. A heat sink utilising plate type fins as TCE is realised wherein a mass reduction factor (MRF) of 1.4 is achieved against traditional approach. This is followed by a heat sink with pin type fins as TCE and a MRF of 2.6 is achieved. Effect of thermal cycling and vibration on its performance is also studied.

Keywords: Hybrid heat sink; Thermal inertia; Phase changing materials; Fins; Transient thermal response

NOMENCLATURE

ρ	Density of the material
$\dot{q}$	Internal heat generation rate per unit volume
c	Specific heat of the material
T	Temperature inside the element
v	Velocity of the element
k	Thermal conductivity of the material
t	Time
x, y, z	Length
q	Heat flux
Q	Heat flow
NPG	Neo Pentyl-Glycol
TCE	Thermal conductivity enhancer
HHS	Hybrid heat sink
BHS	Baseline heat sink
MRF	Mass reduction factor
EMHS	Equivalent mass heat sink
DSC	Differential scanning calorimetry
NI	National instruments

1. INTRODUCTION

Miniaturisation and capability augmentation of electronic components and systems has led to an escalation in their power densities. Depending upon efficiency, a considerable fraction of this power is dissipated in the form of heat. Since natural heat rejection mechanisms namely convection, radiation and conduction are ineffective during launch vehicle flight-due to absence of air at higher altitudes, a relatively small thermal gradient for radiation and mounting of electronics on a non-conductive deck respectively- and active cooling systems are not preferable due to their inherent mass and system complexities and the fact that the systems have to work only for a small duration, electronics systems have to rely on their own thermal capacity to absorb heat to ensure that excessive temperatures are not developed during operation duration. Similar situation tends to occur in the following instances:

(i) Remotely located and intermittently operated avionics on aircrafts and missiles generally have to manage the heat on their own during their operation[1].
(ii) Towards the end of the cruise missiles' flights, when fuel supply runs low, the temperatures may increase. At this point it may be necessary to use the thermal inertia in electronics structure to keep the system cool enough to finish its flight[2].

This inertia is traditionally built-into the system by increasing chassis (support structure) mass proportionally to the associated thermal load. But for power intensive systems, especially in vehicle equipment bay (VEB) stage where mass is at a premium, this results in a mass penalty on the payload capability. Phase changing materials (PCMs) can be utilised for imparting this inertia at a comparatively lower mass penalty, owing to their latent heat absorption capability.

PCMs have long been utilised as basic components of thermal control subsystems in spaceflight applications such as planetary descent probes, satellites and payloads[3-6]. Leoni and Amon[7] investigated the use of PCMs with solid-

Received : 02 August 2016, Revised : 16 April 2018
Accepted : 07 May 2018, Online published : 25 June 2018

liquid phase transformation for transient thermal control of electronic equipment, both analytically and experimentally. Fosset and Kudirka[1] suggested the use of microencapsulated PCMs for aircraft electronics passive cooling. Benson[8], *et al.* studied polyhydric alcohols involving crystalline transformation, for use as thermal energy storage. These polyhydric alcohols were further explored by Wirtz[9-11], *et al.* for use in heat sinks. For thermal control of Li-BCX battery, used as electrical supply source for the astronauts' space suit, Son and Morehouse[12] considered NPG and PG as thermal energy storage materials. ESA's Future Launchers study team projected a payload gain of 13 kg - 15 kg for PCMs utilisation in Ariane 5LV VEB[13]. SpaceX uses PCMs to keep a payload warm, without power for 6 h, during the transfer from the cargo module dragon to an express logistics carrier (ELC) on the space station (ISS)[14].

In the present paper, a trade-off between simplicity and reliability of a conventional heat-sink and storage capability of a PCM based heat-sink has been achieved by utilising dry PCM for launcher avionics thermal control. The durability of this type of heat-sinks against thermal cycling and vibration loads is also demonstrated.

2. PHASE CHANGING MATERIAL

2.1 Solid-Liquid

This type of PCMs (e.g. paraffin wax) pose problem of fluid containment, acceleration and orientation sensitivity. Also, a large volume change takes place when they melt and voids are introduced when they solidify so effective thermal conductivity is reduced. Salt hydrates are generally corrosive, absorb and loose water during phase transition and tend to form partially hydrated crystals, affecting performance. Metallic alloys, though used in military systems[15], have mass densities of an order of magnitude higher than the hydrocarbons resulting in heavier systems. Typical properties of this type of PCMs[16], along with other candidate materials, are as shown in Table 1.

2.2 Liquid-Vapour

Systems employing liquid-vapour transition must accommodate the relatively large specific volume changes that accompany transition.

2.3 Solid-Solid

For these PCMs, liquid phase need not be contained; segregation of components is less likely so packaging difficulties associated with solid-liquid PCMs are avoided. Since there is no fluid phase, the performance of the unit will be independent of inertial loading and system orientation[8].

These PCMs include micro-encapsulated solid-liquid PCMs (effectively dry) and solid-solid organic PCMs (dry). But since encapsulation needs an independent PCM realisation process and heat sink has to be spring loaded so as to compensate for the large volume change, solid-solid PCM are selected for use.

A certain class of polyalcohols (NPG, PG etc.) constitutes tetrahedral molecules with methylol groups and methyl group bonded to the central carbon atom. Planes of these tetrahedral molecules are held together by hydrogen bonds. As the material is heated through the phase transition temperature, the hydrogen bonds begin to break and individual molecules become free to rotate and vibrate about their centres. Because of these additional rotational and vibrational states available, they are able to store thermal energy without any rise in temperature[8]. These materials are non-toxic, cost-effective and non-reactive with chassis material. A polyhydric alcohol named Neopentyl Glycol ($C_5H_{12}O_2$) is identified for use, owing to its desirable transition temperature range [9-11].

3. HEAT SINK DESIGN

The governing differential equation, for a small element of a typical heat sink, can be expressed as follows:

$$\rho c\left(\frac{\partial T}{\partial t}+v_x\frac{\partial T}{\partial x}+v_y\frac{\partial T}{\partial y}+v_z\frac{\partial T}{\partial z}\right)$$
$$=\frac{\partial}{\partial x}\left(k\frac{\partial T}{\partial x}\right)+\frac{\partial}{\partial y}\left(k\frac{\partial T}{\partial y}\right)+\frac{\partial}{\partial z}\left(k\frac{\partial T}{\partial z}\right)+\dot{q} \quad (1)$$

The working principal of a heat sink in launch vehicle differs from the ground-based heat sinks in the sense that it absorbs heat under transient thermal conditions instead of rejecting it under steady-state. The design focus is to limit temperature rise by reducing thermal spreading resistance and increasing thermal absorption capability, at a lower mass penalty. It is traditionally accomplished by using aluminium, albeit at relatively higher mass penalty due to its lower absorption capability. PCM materials can be used to impart this capability but their extremely low thermal conductivity will necessitate an undesirably high temperature gradient for heat distribution, if used alone. To alleviate the problems associated with using either of the materials alone, a hybrid heat sink with aluminium for minimising the spreading resistance (termed TCE) and PCM for maximising storage capability can be employed. The TCE will maximise the PCM exposure to heat-flux and PCM in turn will absorb that heat without any appreciable increase in temperature.

The governing equation (neglecting convection and

Table 1. Physical properties of various candidate PCM[16]

Material type	Transition	Temp. range (°C)	Latent heat (J/cc)	Density (g/cc)
S-S organic compounds (TCC)	S-S (dry)	21 - 100	144 - 212	~1.1
Micro-encap. paraffin (Thermosorb)	S-L (wet)	6 - 101	95 - 186	~0.9
Paraffin (Eicosane)	S-L (wet)	-12 - 71	128 - 197	0.75 - 0.88
Non-paraffin organics (Beeswax)	S-L (wet)	-13 - 187	131 - 438	0.85 - 1.57
Salt hydrates ($MgSO_4 7H_2O$)	S-L (wet)	28 - 137	270 - 650	1.5 - 2.2
Metallics (Eutectic Bi-Cd-In)	S-L (wet)	30 - 125	200 - 800	6 - 10

internal heat generation), for a small hybrid heat sink element (Fig. 1), can now be rewritten as follows:

$$\frac{\partial T}{\partial t} = \left(\frac{k}{\rho c}\nabla^2 T\right)_{TCE} + \left(\frac{k}{\rho c}\nabla^2 T\right)_{PCM} \quad (2)$$

The first and second terms on the RHS represent heat transfer in the TCE and PCM respectively. Since the entire heat is transferred to PCM through TCE (from surface at temperature T0), TCE's conductivity must be high, to ensure that its temperature T1 is close to T0 so that the PCM (at temperature T2) is exposed to a higher temperature, for a particular input heat. This is essential to reduce the overall temperature difference (T0-T2) required to transfer a particular amount of heat to PCM. However since TCE is not contributing appreciably in storage capability, its content should be optimised for a minimum heat-sink mass.

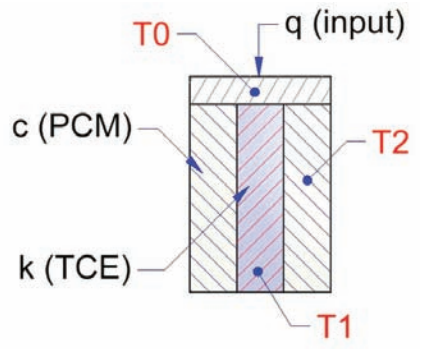

Figure 1. Schematic of a typical HHS element.

4. PLATE-FIN TYPE HEAT SINK (HHS-01)

For capability demonstration, a Heat Sink with plate type fins as TCE is designed, realised and tested as shown in Fig. 2. The heat sink objective is to restrict temperature rise by 70 °C, against a continuous power dissipation of 190 W, for 15 min, on its base plate area (150 x 150 mm^2).

4.1 Thermal Analysis

A non-linear transient thermal analysis is carried out using finite element (FE) method to determine the thermal response of the heat sink wherein lower order hexahedral elements are used for domain discretisation. Only conduction and radiation mode of heat transfer are considered. Thermal conductivity of aluminium alloy and thermal capacity of Neopentyl Glycol (*Alpha Aesar* make) are obtained experimentally (Table 2 and Fig. 3). For including the PCM latent heat in the model, its specific heat (c) is increased around transition range as per the curve obtained from DSC measurement. An interfacial contact resistance of 4x10^{-4} m^{2}K/W between PCM and Aluminium, as identified experimentally by Wirtz[10], *et al.*, is considered. An emissivity of 0.05 is assumed for aluminium external surfaces, to include radiation heat exchange with ambient. A heat-flux of 0.85W/m^2 is applied on the base plate as shown in Fig. 2 to simulate a power of 190 W. The corresponding temperature distribution on heat sink is as shown in Fig. 4. As can be observed, the design objective is met and TCE is almost isothermal on account of its high thermal conductivity.

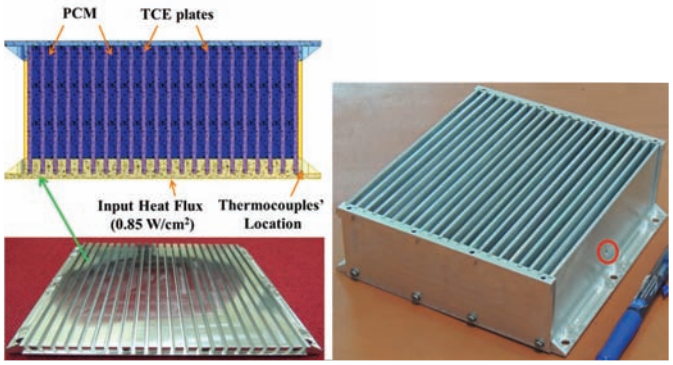

Figure 2. Internal details of plate-fin heat sink along with the realised hardware (level-equalisation hole indicated in red) before PCM pouring.

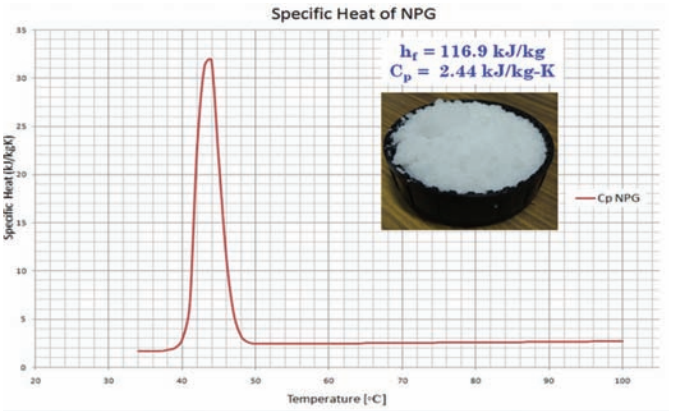

Figure 3. Thermal capacity variation with temperature for neopentyl glycol.

The same analysis is carried out using finite volume (FV) method as well to establish the corresponding merits and demerits of the two, for future use. Both methods produced similar results and even though a finer mesh was warranted in FV based method considering mesh quality requirements, the solution converged faster. However, the modelling, meshing and applying boundary conditions was easier in FE based method so it is selected for future use.

The mass distribution for the heat-sink is as follows:

Heat sink mass : 1960g
Chassis mass : 1530 g (78 % of total mass)
NPG mass : 430 g (22 % of total mass).

4.2 Heat Sink Realisation

The heat sink components are realised by milling as shown in Fig. 2 and then assembled with thermally conductive

Table 2. Physical and thermal properties of materials used in design

Material	Density (kg/m^3)	Specific heat (kJ/kg-K)	Thermal conductivity (W/m-K)	Transition temp. (°C)	Enthalpy of transition (kJ/kg)
AA-6351 (T6)	2705*	0.896	176.8*	--	--
NPG	800*	2.44*	0.1	40-48*	116.9*

* Experimentally determined values

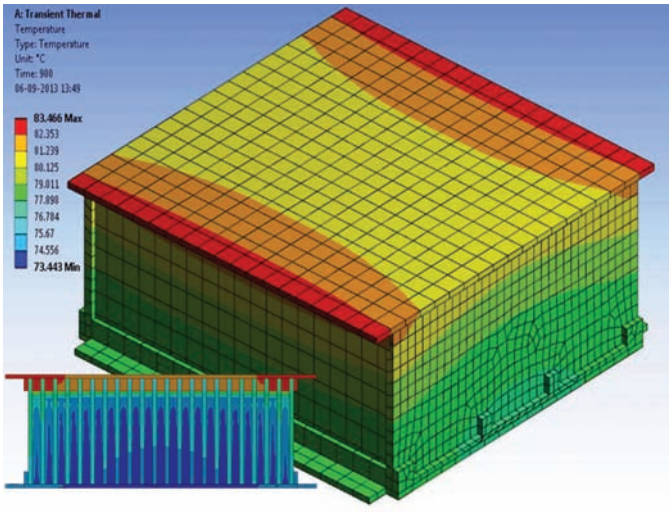

Figure 4. Temperature distribution on and across HHS01 (heat input from top side).

paste applied at interfaces. A small hole is drilled in all TCE plates for enabling molten PCM to flow across the individual cavities formed between these plates for level equalisation. NPG is melted and poured in the cavities created between fins, by making use of two funnels fixed on the holes provided on opposite ends of heat-sink cover. These two funnels, functioning similar to runner and riser in casting process, enable the entrapped air to escape and acted as material reservoir for the heat-sink when the initial molten material shrunk to a very low volume during solidification. To quantify the advantage, an aluminium block with same mass and footprint area as that of heat sink, called baseline heat sink (BHS), is also realised.

4.3 Experimental Set-Up

To validate the design, an experimental set-up comprising of a hot plate (with an auto-transformer for supplying and varying power), a 32-channel, NI based data acquisition system and an insulation box is used. The detail of the experimental set up is as shown in Fig. 5. Heat Sink is kept inside the insulated box leaving the top surface exposed to hot plate.

Thermocouples are mounted at three different locations (Fig. 5) on the heat sink, behind the surface of input heat flux, to monitor its thermal response during experiment. Hot plate, powered by transformer, is fixed on a metal box with built-in provision to cool its sides using water, during experimentation. It is adjusted to supply a uniform flux of 0.85 W/cm^2 to the heat sink by calibrating the electrical power supply with the heat flux sensors placed on the heat sink surface exposed to hot plate. The total measurement uncertainty during the experiment can be attributed to inaccuracies in supplying input heat flux ($\delta q/q = 4$ %), measuring temperature ($\delta T/T = 1$ %), and inadvertent heat leakage ($\delta Q_{loss}/Q = 5$ %) which is estimated to be 6.5 per cent, by using Eqn. (3).

$$U_{exp.} = \sqrt{\left(\frac{\partial T}{T}\right)^2 + \left(\frac{\partial q}{q}\right)^2 + \left(\frac{\partial Q}{Q}\right)^2} \times 100\% \qquad (3)$$

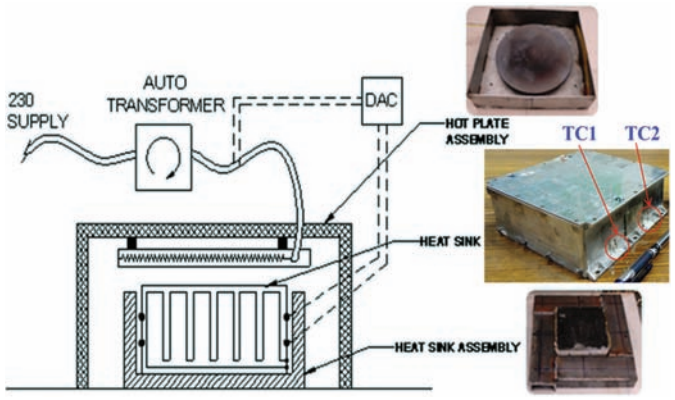

Figure 5. Test setup with 3 thermocouples mounted on bottom side of heated surface (TC1, TC2 shown; TC3 on opposite side).

The experiment is conducted for around 21 min and the temperature rise with course of time is monitored. Since the reported temperature values, by all the thermocouples are quite close to each other, their average value is taken as reference for making any comparisons. To quantify the advantage of using this heat sink, same experiment is conducted on BHS.

As can be seen from the Fig. 6, the predicted response is comparable to experimental results. The aberration in results can be attributed to test uncertainties and variations in PCM thermal behaviour and contact resistance. Heat sink maintains the temperature below design limit successfully for 15 min while baseline design exceeds the design limit of 95 °C (70 °C rise from 25 °C) at about 11 min from start of operation. The advantage can be expressed in terms of either of two parameters i.e. increase in workable time or mass saving. The workable time is increased by a factor of 1.36 while a MRF (mass-ratio of BHS and HHS for same thermal performance) of 1.4 could be achieved.

5. PIN-FIN TYPE HEAT SINK (HHS-02)

For MRF enhancement, pin type fins were identified for

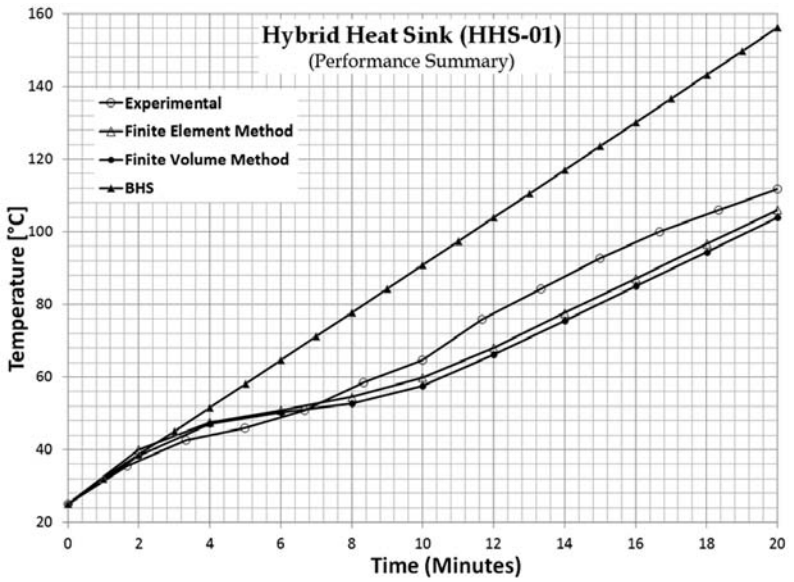

Figure 6. Comparison of experimental and computed thermal response for HHS-01.

use as TCE since they distribute heat more uniformly-attributable to an efficient three-dimensional heat diffusion[17-18]. The design objective for this hybrid heat sink (HHS-02) is set to limit the temperature rise by 50 °C for a heat flux of 0.25 W/cm^2 for 30 min.

Transient thermal analysis with same material properties, boundary conditions and modelling strategy as adopted in HHS-01 is carried out for an operation duration of 30 min, for its mass optimisation and final thermal response prediction. For optimisation, design of experiments (DOE) based approach is utilised, with overall mass minimisation as an objective function, temperature limit as constraint, and TCE and PCM content as design variables. Since for a given TCE content, smaller fin cross-section (in turn higher number of fins) will result in a uniform heat distribution thereby improving heat sink performance size, smallest feasible size of 2x2 mm^2, based on manufacturing constraints, is selected. The parameter fin-to-fin spacing (range: 1-6 mm), with number of fins identified by equi-distributing them on entire footprint, is used to vary the relative content of TCE and PCM in a fixed total volume determined by foot-print area and height wherein the fraction of total volume left empty by TCE is assigned as PCM by making use of boolean operations. By using screening optimisation algorithm on the response curve generated by the DOE, a volume fraction of 10 TCE - 90 PCM is obtained. This value is comparable to the reported values for systems with similar thermal conductivity combinations[17-18]. Final mass distribution, after including side walls, cover and mounting provision is shown as follows:

Heat sink mass : 530 g
Chassis mass : 270 g (51 % of total mass)
NPG mass : 260 g (49 % of total mass)

A maximum temperature of 67 °C at the end of performance span is predicted for the optimised design. The temperature variation across the heat sink is plotted in Fig. 7.

Same experimental set-up, as that for HHS-01 is used for its performance validation with hot plate recalibrated to supply a heat flux of 0.25 W/cm^2. BHS for HHS-02 as well as an equivalent mass heat sink (EMHS) i.e. solid aluminium block with 2.6 times more mass than that of HHS-02 are also tested under identical thermal conditions. To study the impact of thermal cycling, the experiment was repeated 10 times with a gap of 24 h between successive tests. Afterwards, the heat sink was subjected to standard design qualification vibration levels (10 g Sine, 13.5 g_{rms} random, and 50 g shock), followed by the same thermal test. The variation in observed thermal response during all of these tests is within the test set-up uncertainty.

As evident from Fig. 8, HHS-02 maintains the temperature below design limit successfully for 30 minutes. Also, the workable time is more than tripled while a MRF of 2.6 could be achieved.

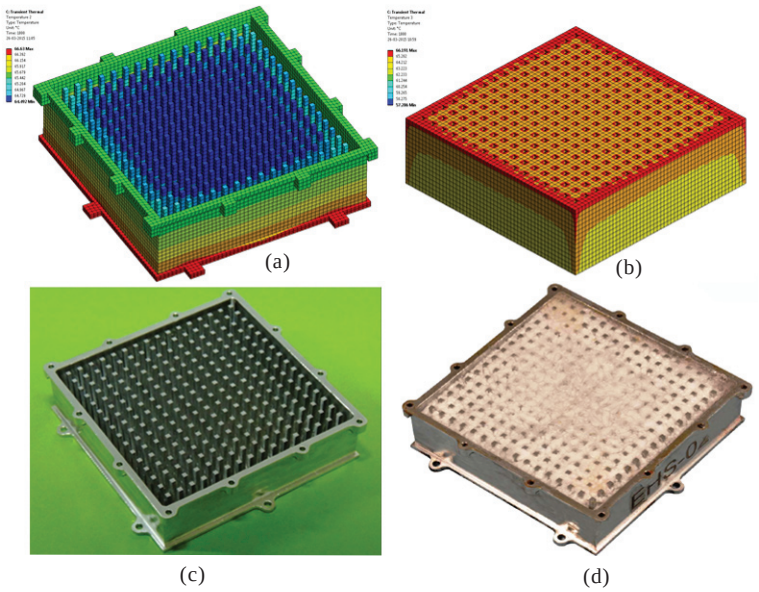

Figure 7. (a) Temperature distribution on heat sink and (b) enclosed NPG brick (c) HHS-02 before and (d) after PCM pouring.

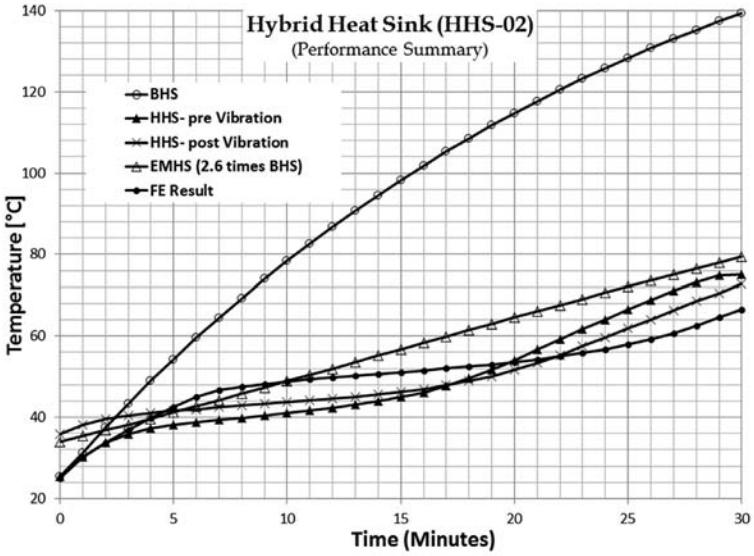

Figure 8. Comparison of experimental thermal response for HHS-02 and baseline design.

6. CONCLUSIONS

To tackle the design concerns arising out of ever increasing power dissipation levels of electronic components and systems in launch vehicles, heat sinks utilising crystalline transformation energy of NPG material have been designed. Two different TCE configurations, to compensate for low thermal conductivity of NPG, are studied. MRF of 1.4 and 2.6 is achieved for plate-fin and pin-fin type heat sinks respectively. This heat sink operates passively, reversibly and is inherently reliable. It can be employed in power intensive systems like RADAR, transmitter, power amplifiers and electromechanical actuators. Other potential applications include chip level thermal management and passive thermal control of satellite payloads in conjunction with active systems.

REFERENCES

1. Fossett, A.J.; Maguire, M.T.; Kudirka, A.A.; Mills, F.E. & Brown, D.A. Avionics passive cooling with

microencapsulated phase change material. *J. Electron. Packag*., 1998, **120**(3), 238-242. doi: 10.1115/1.2792628
2. Steinberg, Dave S. Cooling techniques for electronic equipment. John Wiley & Sons Inc., US, 1991, pp. 7.
3. Kirkpatrick, J.P. & Brennan, P. J. The advanced thermal control flight experiment. *In* AIAA 8th Thermophysics Conference, California, 1973, pp. 1-11. doi: 10.2514/6.1973-757
4. Abhat, A. & Groll, M. Investigation of phase change material (PCM) devices for thermal control purposes in satellites. *In* AIAA/ASME Thermophysics and Heat Transfer Conference, Massachusetts, 1974, pp. 1-9. doi: 10.2514/6.1974-728
5. Brennan, P.J.; Suelau, H.J. & McIntosh, R. Development of a low temperature phase change material package. *In* AIAA 12th Thermophysics Conference, Albuquerque, 1977, pp. 1-5. doi: 10.2514/6.1977-762
6. Morey, T. F. & Gorman, D. N. Development of the Viking Mars lander thermal control subsystem design. *J. Spacecraft*, 1976, **13**(4), 229-236. doi: 10.2514/3.57082
7. Leoni, M. & Amon, C. H. Thermal design for transient operation of the TIA wearable portable computer. *In* The Pacific Rim/ASME International Intersociety Electronic and Photonic Packaging Conference, Hawaii, 1997, pp. 2151-2162.
8. Benson, D.K.; Burrows, R.W. & Webb, J.D. Solid state phase transitions in pentaerythritol and related polyhydric alcohols. *Solar Energy Mater.*, 1986, **13**(2), 133-152. doi: 10.1016/0165-1633(86)90040-7
9. Wirtz, R.A.; Zheng, Ning & Chandra, Dhanesh. Thermal management using 'dry' phase change materials. *In* Semiconductor Thermal Measurement and Management Symposium, San Diego, 1999, pp. 74-82. doi: 10.1109/STHERM.1999.762432
10. Wirtz, R.A. & Zheng, Ning. A hybrid thermal energy storage device, Part 1: Design Methodology. *J. Electron. Packag.*,2004, **126**(1), 1-7. doi: 10.1115/1.1646419
11. Wirtz, R.A. & Zheng, Ning. A hybrid thermal energy storage device, Part 2: Thermal performance figures of merit. *J. Electron. Packag.*, 2004, **126**(1), 8-13. doi: 10.1115/1.1646420
12. Son, C.H. & Morehouse, J.H. Thermal conductivity enhancement of solid-solid phase change materials for thermal storage. *J. Thermophysics*, 1991, **5**(1), 122-124. doi: 10.2514/3.237
13. Collete J.P.; Rochus, P.; Peyrou-Lauga, R.; Ramusat, G.; Pin, O.; Nutal, N. & Crahay, J. Advanced thermal control of launcher equipment bay using phase change material. *In* International Astronautical Congress IAC-13 C2,8,7x18233, 2013, pp. 1-14.
14. Michael K. Choi. Using paraffin with -10 °C to 10 °C melting point for payload thermal energy storage in SpaceX dragon trunk. *In* 11th International Energy Conversion Engineering Conference, San Jose, 2013, pp. 1-7. doi: 10.2514/6.2013-4099
15. Antohe, B.V.; Lage, J.L.; Price, D.C. & Weber, J.L. Thermal management of high frequency electronic systems with mechanically compressed microporous cold plates. *In* ASME National Heat Transfer Conference, 1996, pp. 179-186.
16. Lane, G.A. *Editor*, Solar heat storage and latent heat of materials, CRC Press Inc., Boca Raton FL. 1983.
17. Nayak, K.C.; Saha, S.K.; Srinvasan, K. & Dutta, P. A numerical model for heat sinks with phase change materials and thermal conductivity enhancers. *Int. J. Heat Mass Transfer*, 2006, **49**, 1833-1844. doi: 10.1016/j.ijheatmasstransfer.2005.10.039
18. Baby, R. & Balaji, C. Experimental investigations on phase change material based finned heat sinks for electronic equipment cooling. *Int. J. Heat Mass Transfer*, 2012, **55**, 1642-1649. doi: 10.1016/j.ijheatmasstransfer.2011.11.020

ACKNOWLEDGMENTS

Authors sincerely appreciate the guidance of Mr Pradeep Kumar, Group Director (CASG/AVN/VSSC) and Mr Mookiah T, Deputy Director (AVN/VSSC) for this work. Authors would also like to place on record, their gratitude towards Shri Manoj VS (AMFF/VSSC) for rendering his support in realisation of the heat sink and Shri Rakesh Ranjan (PCM/VSSC) for carrying out thermo-physical characterisation of the materials.

CONTRIBUTORS

Mr V.K. Sen received his BTech (Mechanical Engineering) from Himachal Pradesh University, Shimla. Presently involved in structural and thermal design in Avionics Mechanical Fabrication Facility, Vikram Sarabhai Space Centre, Trivandrum.
In the current study, he has contributed towards PCM identification and heat sink designs.

Mr J. Jaiswal received his BTech (Aerospace Engineering) from Indian Institute of Space Science and Technology, Trivandrum. Presently involved in structural and thermal design in Avionics Mechanical Fabrication Facility, Vikram Sarabhai Space Centre, Trivandrum.
In the current study, he has contributed towards thermal analysis and performance optimisation of the designs.

Mr A. Nandi received his BE (Mechanical Engineering) from North Bengal University, West Bengal. Presently heads the structural and thermal design section in Avionics Mechanical Fabrication Facility, Vikram Sarabhai Space Centre, Trivandrum.
In the current study, he has contributed towards fabrication of mechanical elements of Heat Sinks.

Mr A.V. Aliyas received his BTech in Mechanical Engineering from N.S.S. College of Engineering, Calicut University. Presently heads Avionics Mechanical Fabrication Facility, Vikram Sarabhai Space Centre, Trivandrum.
In the current study, he has contributed towards assembly of heat sink and vibration and thermal cycling tests.

Mr A. Pillai received his BTech (Mechanical Engineering) from N.S.S. College of Engineering, Calicut University and ME (Mechanical Engineering) from Indian Institute of Science, Bangalore. Presently the Group Head of Propulsion and Plasma Research Group, Vikram Sarabhai Space Centre, Trivandrum.
In the current study, he has contributed towards the setting up of test rig and conducting performance testing of the heat sinks.